HHS Public Access

Author manuscript

Int Conf Virtual Rehabil. Author manuscript; available in PMC 2016 October 04.

Published in final edited form as:

Int Conf Virtual Rehabil. 2015 June ; 2015: 30–37. doi:10.1109/ICVR.2015.7358598.

A Closed-loop Brain Computer Interface to a Virtual Reality Avatar: Gait Adaptation to Visual Kinematic Perturbations

Trieu Phat Luu, **Yongtian He**, **Samuel Brown**, **Sho Nakagome**, and **Jose L. Contreras-Vidal [IEEE Senior Member]**

Department of Electrical and Computer Engineering, University of Houston, Houston, TX 77004, USA

Abstract

The control of human bipedal locomotion is of great interest to the field of lower-body brain computer interfaces (BCIs) for rehabilitation of gait. While the feasibility of a closed-loop BCI system for the control of a lower body exoskeleton has been recently shown, multi-day closed-loop neural decoding of human gait in a virtual reality (BCI-VR) environment has yet to be demonstrated. In this study, we propose a real-time closed-loop BCI that decodes lower limb joint angles from scalp electroencephalography (EEG) during treadmill walking to control the walking movements of a virtual avatar. Moreover, virtual kinematic perturbations resulting in asymmetric walking gait patterns of the avatar were also introduced to investigate gait adaptation using the closed-loop BCI-VR system over a period of eight days. Our results demonstrate the feasibility of using a closed-loop BCI to learn to control a walking avatar under normal and altered visuomotor perturbations, which involved cortical adaptations. These findings have implications for the development of BCI-VR systems for gait rehabilitation after stroke and for understanding cortical plasticity induced by a closed-loop BCI system.

Keywords

Brain machine interface; visuomotor adaptation; virtual environment; gait adaptation

I. Introduction

Spinal cord injury (SCI) and stroke are the leading causes of long-term disability around the world. In the United States, more than 795,000 people have a stroke every year [1], and the number of people who have SCI is estimated to be 276,000 [2]. Gait deficit is a debilitating outcome from stroke and SCI. Therefore, restoration of gait function is crucial and it has been a long-standing focus in rehabilitation research.

Walking is a complex task and its quality is usually determined by a smooth and symmetric walking gait pattern. However, patients with cerebral damage from stroke often adopt asymmetric walking patterns [3,4]. Prior studies of gait adaptation to a spit-belt perturbation, which creates asymmetric walking, demonstrated that temporal and spatial control for symmetric gait can be adapted separately [5]. Moreover, the understanding of motor adaptation mechanisms may suggest appropriate intervention for gait rehabilitation. Analyses of aftereffects following split-belt treadmill adaptation showed that the walking

adaptation partially transfers to over-ground walking in patients post-stroke. This could imply that the persistence of improved symmetry can be used in gait restoration in post-stroke gait rehabilitation [6]. The advantages of visuomotor adaptation in improving task performance in patients post-stroke have also been demonstrated [7,8].

Rehabilitation based on Virtual Reality (VR) (or Virtual Environments, VE) is an emergent area of research that provides several advantages to the patients and researchers [9,10]. Some of the advantages of using VR are its interactivity and its tendency to motivate subjects. VE creates an interactive environment that immerses the user in the experimental setting. This is important in rehabilitation to ensure patient's engagement and motivation to improve performance [11]. Applications of VR/VE in rehabilitation as growing; for example, a virtual reality soccer game was used to improve walking performance for pediatric rehabilitation [12]. Another study showed the advantages of using VR in gait rehabilitation by creating an obstacle avoidance VE system during walking in chronic post-stroke patients [13]. Moreover, there are a few randomized controlled trial (RCT) studies that assessed the use of VR during stroke rehabilitation. A Cochrane review has reported that there was not enough evidence to conclude the effectiveness of VR compared to the conventional therapy in improving gait speed [14]. On the other hand, Yang *et al.* reported that VR could be beneficial for gait rehabilitation [15]. Llorens *et al.* conducted a RCT study on improving balance during gait using VR with chronic stroke patients [16]. Interestingly, some research showed that a VR intervention is effective on triggering cortical reorganization and associated locomotor recovery [17].

Although locomotor adaptation, visuomotor adaptation and VR-based neurorehabilitation have been used to improve motor function, surprisingly little is known about the neural mechanisms of locomotor recovery [18] [19]. Previous studies of functional near-infrared spectroscopy (fNIRS) have shown the involvement of frontal, premotor and supplementary motor areas during walking [20]. In addition, functional magnetic resonance imaging (fMRI) studies have demonstrated that treadmill exercise alters brain activation of paretic leg movements in stroke patients, evoking new connections at the subcortical and cerebellar levels [21]. These brain activation changes are associated with improved walking function after treadmill training, which also positively affects spatio-temporal gait parameters during over-ground walking [22]. The use of transcranial magnetic stimulation (TMS) shows that brief exposures to treadmill walking altered corticospinal excitability to lower extremities in chronic stroke survivors [23]. However, these approaches lack the temporal resolution required to uncover the time course of the cortical contributions to the control of gait.

Neural engineering approaches to the study and restoration of gait function have demonstrated the possibility of reconstructing gait kinematics from patterns of cortical activity acquired via intracortical electrode arrays in non-human primates [24] and non-invasive scalp electroencephalography (EEG) in human subjects [25] with the same accuracy (for a review see [26]). More recently, Bulea *et al.* decoded sit-to-stand and stand-to-sit movements from EEG signals recorded immediately prior to those actions suggesting EEG can be used to predict locomotive and non-locomotive actions [27]. Moreover, Kilicarslan *et al.* pioneered the deployment of EEG-based BCI systems to control lower-body powered robotic exoskeletons by subjects with SCI [28]. Applications of BCI systems for gait

rehabilitation using VR/VE represent a new form of personalized neuro-rehabilitation based on putative shared brain networks involved in action observation and action execution (for a review see [29]). However, little is known about brain networks adapt during gait adaptation based on BCI-VR systems.

In this study, an EEG-BCI system based on the unscented Kalman filter has been designed to infer lower limb joint angles during treadmill walking in real-time from EEG signals in healthy subjects. The predicted lower limb joint angles were used to control a walking avatar in a virtual environment, thereby closing the loop through the brain. Virtual kinematic perturbations of the subject's walking patterns were also introduced to investigate the changes in brain activity to gait during adaptation using the closed-loop BCI-VR. The virtual kinematic perturbations resulted in an asymmetric walking pattern of the walking avatar. We hypothesized that with practice the subjects can gain more BCI control and reduce the gait asymmetry of the walking avatar through EEG signals.

II. Materials and Methods

A. Experimental Setup and Procedure

Two healthy male subjects, aged 23 with no history of neurological disease or lower limb pathology participated in this study. All participants provided voluntary consent and performed study procedures that were approved by the Institutional Review Board at the University of Houston. Each subject participated in eight trials, which are identical but happened on different days. The full protocol usually lasted less than an hour. Except for a short period of standing still in the beginning and end, the subject walked on a treadmill at a fixed speed of 1 mile/hour (mph). A display was placed in front of the treadmill, displaying an avatar of the subject standing/walking in a straight hallway VE (Fig. 2A). Only body parts below waist were shown on the screen, because only lower limb movements were studied. During baseline performance, the avatar followed the movement of the subject precisely in real-time by matching the joint angles on hip, knee, and ankle on both legs. These angles were measured using six goniometers, one on each joint, measuring angles in the sagittal plane.

As illustrated inFig. 1, each trial began with the subject standing still on the treadmill for 2 minutes. The treadmill was then slowly sped up to 1 mph by the experimenters. The subject was able to see the avatar following his/her movement correctly. The first 15 minutes of walking served as a baseline condition, in which the subject also got familiar with the VE. In this article, we call this the *gonio-control* phase. The parameters of the unscented Kalman filter were updated every minute in this phase. A detailed description of this algorithm is provided in Section II. D and E. The *gonio-control* phase was followed by an *EEG-control* phase, in which the right hip, knee, and ankle joints of the avatar followed the outputs of the real-time BCI decoder instead of the goniometers. The *EEG-control* phase consists of three parts: pre-exposure (8 mins), exposure (15 mins), and post-exposure (8 mins). During the exposure time, a visual-kinematic perturbation was introduced into the avatar: all joint angles on the right leg of the avatar were linearly scaled down into 70% of original value. All subjects were briefly informed before the experiment that there would be *gonio-control, EEG-control* and perturbation, but details of the protocol were not revealed. They were

instructed to correct the avatar's gait pattern once any abnormality is noticed. Meanwhile, they continued to walk on the treadmill during all phases. In the end, the trial terminated after the subject stood still on the treadmill for another 2 minutes.

B. Data Collection

Whole scalp 64-channel active EEG data were collected (actiCap system, Brain Products GmbH, Germany) and labeled in accordance with the extended 10–20 international system. EEG data were online referenced to channel FCz. The sampling rate was 100 Hz. Goniometer data (SGI 50 & SG110/A Gonio electrodes, Biometrics Ltd, UK) were also sampled at 100 Hz, and recorded in sync with EEG data using our own software.

Three wireless OPAL sensors (OPAL, APDM Inc., Portland, OR) were mounted on the head, left heel, and right heel of the subject. Each sensor included accelerometer, gyroscope, and magnetometer sampled at 128Hz. The sensor on head was used to rule out possibility that EEG may be contaminated by motion artifacts. The other two sensors on the feet provided timing for the gait cycles (seeFig. 2B). OPAL data was synchronized with EEG and goniometer data. A raster plot showing these three modalities of data are shown inFig. 2C.

C. Signal Pre-processing

All processing was carried out in custom C++ software in real-time. Peripheral EEG channels were immediately removed as they are most susceptible to artifacts from eye-blinks, head movements, and facial/cranial muscle activity .Removed channels are labeled with a red "x" inFig. 2A. EEG data were band-pass filtered at 0.1–3 Hz (delta band), and then normalized to the same scale (zscore). Studies show that delta band EEG contains intended movement-related information, in particularly for lower limb BCI [25,30]. Joint angles from goniometers were low-pass filtered at 3 Hz also in real-time. Because subjects walked at a very slow speed (1 mph), the 0–3 Hz band covers most power in joint angle signals [31].

D. Unscented Kalman Filter Decoder

Linear decoders such as Wiener filters and Kalman filters are most commonly used in BCI applications [32]. However, these models cannot handle a non-linear relationship between neural activities and limb movements. Recently, Li *et al.* showed that the unscented Kalman filter (UKF) outperformed the Kalman filter and the Wiener filter in both offline and real-time BCI operation [33], and thus, we adopted the UKF as the decoder for the BCI-VR system.

E. Online Updates of UKF Parameters

BCI decoders are typically trained offline by fitting neural signals against kinematic data. During closed-loop BCI, the subjects can alter their neural activity and affect the accuracy of the trained decoder which does not account for the difference in neural activity. Recently, Orsborn *et al.* showed that closed-loop decoder adaptation (CLDA) where decoder parameters are updated during closed-loop can yield performance improvements [34]. To apply CLDA for UKF decoder in this study, the pre-processed EEG and lower limb joint angles were first streamed to a buffer. The buffer size was pre-defined to store 1 minute of

collected data (6000 samples).Fig. 3 depicts the neural decoder steps in the BCI-VR system based on [32] and [33].

III. Results

EEG signals were first analyzed by mean, standard deviation (STD), and signal to noise ratio (SNR). These values were calculated from sliding windows with window size of 30s and step size of Is. EEG artifacts from stereotypical (e.g. eye blinks) and non-stereotypical (e.g. movement, muscle bursts) were removed using Artifact Subspace Reconstruction (ASR) method which is available as a plug-in for EEGLAB software [35]. The output from ASR method and EEG raw data were used to calculate SNR values. The results were grouped based on EEG sensor locations: peripheral (PERI), Frontal (F), Central (C), and Posterior (P) electrodes. The analysis of EEG data and r-values between decoder outputs and lower limb joint angles of subject S2 across 8 days (trials) are shown inFig. 4.

Our decoding method was able to predict lower limb joint angles in the sagittal plane from scalp EEG signals. To quantify the level of accuracy for real-time decoding of lower limb joint angles, the Pearson's *r* values between measured and predicted joint angles were computed for *EEG-control* phase.Table I reports the mean and standard deviation (STD) of Pearson's *r* values for lower limb joint angles decoding of all subjects across all days. In general, the r-values for knee joint angle were higher than for hip and ankle joint angles of both subject SI and S2. *r*-values for knee joint angles were significantly improved after 8 days (e.g., Subject SI: from 0.34± 0.14 to 0.51± 0.10 and subject S2: from 0.14± 0.12 to 0.48± 0.09). In the best cases, the real-time decoder were able to reach the accuracy r=0.51 ± 0.10 (SI, knee joint) and r=0.51 ±0.08 (S2, knee joint).

We observed changes in both actual and predicted gait patterns as subjects adapted to the visual perturbation.Fig. 5A depicts mean and standard deviation (STD) of actual and predicted lower limb joint angles of the right leg during *gonio-control*, pre-, early-, late- and post-exposure for one day. In the *gonio-control* phase, the subject's walking pattern was consistent and STD values of lower limb joint angles were small. However, in early-exposure, the sudden introduction of the visual perturbation resulted in increased STD values. By late-exposure, the STD values were decreased and the subject's walking gait pattern was more stable. The differences between predicted and actual joint angles increased during early-exposure. However, the predicted joint angles were close to the actual joint angles in late- and post-exposure.

The quality of the prediction of lower limb joint angles from EEG signals is shown inFig. 5B. The plot shows an example of the actual and predicted 3D trajectories of lower limb joint angles for day 4 of subject SI. As can be seen, the predicted trajectories became closer to the actual trajectories from pre- to late-exposure stage demonstrating visuomotor adaptation.

Pearson's *r* values between predicted lower limb joint angles in each phase and measured angles in *gonio-control* phase (baseline) were calculated across all days to assess the subjects' performance in controlling the avatar. The median and third quartile of *r* values are

depicted in polar plot inFig. 5C. Statistical analysis (t-test, significance level α=0.05) was also performed. The results showed that *r* values in *gonio-control* phase of the first day are significantly smaller than those of the last day (p=0.027 for SI and p=0.021 for S2). A similar result was found in *post-exposure* phase for subject S2 (p<0.001).

Gait symmetry provides information about the control of human walking. Analyzing gait symmetry is clinically significant and it may have a role in helping clinicians make decisions [36]. In general, there are two components that determine a symmetry metric: an equation to calculate gait symmetry and the spatio-temporal gait parameters used in the equation (e.g. stride length, step length, range of motion, cadence, stance time, swing time, etc) [37]. The symmetry ratio (SR) and range of motion (ROM) of the avatar's lower limbs were used to calculate gait symmetry and thus, the quality of EEG-based avatar control.

$$SR_g = \frac{ROM_{r,g}}{ROM_{l,g}} \quad (1)$$

where g represents the hip, knee or ankle joints; r, and 1 are right and left legs.

SR scores are reported inTable II. Phase 1 is when the avatar was under *gonio-control*. Phases 2 to 5 are early-, pre-, late- and post-exposure, respectively. As can be seen, SR values are close to 1 during phase 1, and significantly decreased at phase 2 when the avatar was under *EEG-control*. Overall, SR values continue to decrease during phases 3 and 4, and increase during phase 5.

IV. Discussion

In this study, a neural decoder was designed to translate neural activity acquired via scalp EEG into lower limb movements in real time. The predicted joint angles were used to control a walking avatar in a virtual environment. Virtual kinematic perturbations of gait patterns in healthy subjects were also introduced to investigate cortical adaptations during gait adaptation using a closed-loop BCI.

Asymmetric walking gait patterns are commonly found in patients post-stroke. Study of walking adaptation to a split-belt perturbation, which creates early asymmetric walking, demonstrated that with practice, subjects can improve phasing and reduce gait asymmetry [5]. Moreover, the understanding of gait adaptation may suggest appropriate interventions for gait rehabilitation. In this study, a closed-loop BCI was used to investigate if changes in brain activity contribute to gait adaptation during virtual kinematic perturbation of a walking avatar in a virtual environment. The results show that the visual kinematic perturbation affected the walking gait patterns of both the subjects and the walking avatar. Interestingly, with practice the subjects gained more control of the walking avatar and improved gait symmetry suggesting the BCI-avatar system triggered cortical plasticity. We found that decoding accuracies (or r-values) varied with mean, STD and SNR scores of the EEG signals, suggesting that signal stability within and across days may be influenced by global internal states of the subjects such as attention, motivation and fatigue.

We also observed that the subjects were able to adapt the avatar's gait patterns controlled via the BCI. This suggests that the visuomotor adaptation can be triggered directly from brain activity and thus the proposed system can also be used as a platform to examine cortical plasticity in the human brain. Studies have shown the CNS's capacity to adapt its structural organization after the development of a brain lesion [38]. Such brain lesion can also be simulated in our settings by deliberately removing certain EEG channels that go to the decoder. With such change, decoder performance is expected to drop and trigger neural adaptation to restore function.

Besides, observational therapy in stroke rehabilitation has been found to be beneficial. In a typical observational therapy, persons with stroke observe a video clip or other people demonstrating a movement before they try it by themselves. Reports suggest that patients with observational therapy show significant improvement in functional assessment, including fMRI, before and after the treatment [39]. Inspired by this fact, we propose to enhance patient involvement by forcing them to use their neural activity to control an avatar instead of passively watching movement from other people. In fact, we also looked at how visual disruption affected the *gonio-control* phase. A clear adapting phase and learning curve can be seen during the perturbation, showing that the subjects were actively learning the new motor coordination skills.

Preliminary results showed that motion artifacts due to walking were minimal at slow speed (1 mph). Since peripheral channels are mainly affected by eye blinks and muscle artifacts, they were removed at data preprocessing. The lack of real-time artifact removal techniques is one of the limitations in this study and it is considered as future work. Further analysis is required in this regard. Neural decoders play a central role in BCI applications. Improving the performance and accuracy of the decoder is an important part in future research. This could be done by analyzing and selecting optimal EEG channels, improving the SNR, and examining the history of EEG data that has the best correlation with kinematic data. EEG source localization will also be important to understand the neural sources of cortical plasticity during BCI learning and during gait adaptation.

Acknowledgments

The authors would like to thank Fangfei Zhang and Jeffrey Gorges for their assistance with the data collection.

This research was supported by award R01NS075889 from the National Institute Of Neurological Disorders And Stroke (NINDS). The content is solely the responsibility of the authors and does not necessarily represent the official views of the NINDS or the National Institutes of Health (NIH).

References

1. Centers for Disease and Prevention. Stroke Facts. 2014 Jan. Available: http://www.cdc.gov/stroke/facts.htm
2. National Spinal Cord Injury Statistic Center. Spinal Cord Injury (SCI) Facts and Figures at a Glance. 2013 Jan. Available: https://www.nscisc.uab.edu/PublicDocuments/fact_figures_docs/Facts%202014.pdf.
3. Hsu A-L, Tang P-F, Jan M-H. Analysis of impairments influencing gait velocity and asymmetry of hemiplegic patients after mild to moderate stroke. Archives of physical medicine and rehabilitation. 2003; 84:1185–1193. [PubMed: 12917858]

4. Lamontagne A, Fung J. Faster is better implications for speed-intensive gait training after stroke. Stroke. 2004; 35:2543–2548. [PubMed: 15472095]
5. Malone LA, Bastian AJ, Torres-Oviedo G. How does the motor system correct for errors in time and space during locomotor adaptation? Journal of neurophysiology. 2012; 108:672–683. [PubMed: 22514294]
6. Reisman DS, Wityk R, Silver K, Bastian AJ. Split-belt treadmill adaptation transfers to overground walking in persons poststroke. Neurorehabilitation and neural repair. 2009; 23:735–744. [PubMed: 19307434]
7. Patton JL, Stoykov ME, Kovic M, Mussa-Ivaldi FA. Evaluation of robotic training forces that either enhance or reduce error in chronic hemiparetic stroke survivors. Experimental Brain Research. 2006; 168:368–383. [PubMed: 16249912]
8. Rossetti Y, Rode G, Pisella L, Farné A, Li L, Boisson D, et al. Prism adaptation to a rightward optical deviation rehabilitates left hemispatial neglect. Nature. 1998; 395:166–169. [PubMed: 9744273]
9. Bohil CJ, Alicea B, Biocca FA. Virtual reality in neuroscience research and therapy. Nat Rev Neurosci. 2011; 12:752–762. 12//print. [PubMed: 22048061]
10. Holden MK. Virtual environments for motor rehabilitation: review. Cyberpsychol Behav. 2005 Jun. 8:187–211. discussion 212-9. [PubMed: 15971970]
11. Rizzo A, Kim GJ. A SWOT analysis of the field of virtual reality rehabilitation and therapy. Presence: Teleoper. Virtual Environ. 2005; 14:119–146.
12. Brutsch K, Schuler T, Koenig A, Zimmerli L, Koeneke SM, Lunenburger L, et al. Influence of virtual reality soccer game on walking performance in robotic assisted gait training for children. J Neuroeng Rehabil. 2010; 7:15. [PubMed: 20412572]
13. Jaffe DL, Brown DA, Pierson-Carey CD, Buckley EL, Lew HL. Stepping over obstacles to improve walking in individuals with poststroke hemiplegia. J Rehabil Res Dev. 2004 May.41:283–292. [PubMed: 15543446]
14. Laver K, George S, Thomas S, Deutsch JE, Crotty M. Cochrane review: virtual reality for stroke rehabilitation. Eur J Phys Rehabil Med. 2012 Sep.48:523–530. [PubMed: 22713539]
15. Yang Y-R, Tsai M-P, Chuang T-Y, Sung W-H, Wang R-Y. Virtual reality-based training improves community ambulation in individuals with stroke: A randomized controlled trial. Gait & Posture. 2008; 28:201–206. 8//. [PubMed: 18358724]
16. Llorens R, Gil-Gomez JA, Alcaniz M, Colomer C, Noe E. Improvement in balance using a virtual reality-based stepping exercise: a randomized controlled trial involving individuals with chronic stroke. Clin Rehabil. 2015 Mar.29:261–268. [PubMed: 25056999]
17. You SH, Jang SH, Kim YH, Hallett M, Ahn SH, Kwon YH, et al. Virtual reality-induced cortical reorganization and associated locomotor recovery in chronic stroke: an experimenter-blind randomized study. Stroke. 2005 Jun.36:1166–1171. [PubMed: 15890990]
18. Butler C, Darrah J. Effects of neurodevelopmental treatment (NDT) for cerebral palsy: an AACPDM evidence report. Dev Med Child Neurol. 2001 Nov.43:778–790. [PubMed: 11730153]
19. Page SJ, Levine P, Sisto S, Bond Q, Johnston MV. Stroke patients' and therapists' opinions of constraint-induced movement therapy. Clin Rehabil. 2002 Feb.16:55–60. [PubMed: 11837526]
20. Harada T, Miyai I, Suzuki M, Kubota K. Gait capacity affects cortical activation patterns related to speed control in the elderly. Exp Brain Res. 2009 Mar.193:445–454. [PubMed: 19030850]
21. Luft AR, Macko RF, Forrester LW, Villagra F, Ivey F, Sorkin JD, et al. Treadmill exercise activates subcortical neural networks and improves walking after stroke: a randomized controlled trial. Stroke. 2008 Dec.39:3341–3350. [PubMed: 18757284]
22. Patterson SL, Rodgers MM, Macko RF, Forrester LW. Effect of treadmill exercise training on spatial and temporal gait parameters in subjects with chronic stroke: a preliminary report. J Rehabil Res Dev. 2008; 45:221–228. [PubMed: 18566940]
23. Forrester LW, Hanley DF, Macko RF. Effects of treadmill exercise on transcranial magnetic stimulation-induced excitability to quadriceps after stroke. Arch Phys Med Rehabil. 2006 Feb. 87:229–234. [PubMed: 16442977]

24. Fitzsimmons NA, Lebedev MA, Peikon ID, Nicolelis MA. Extracting kinematic parameters for monkey bipedal walking from cortical neuronal ensemble activity. Frontiers in integrative neuroscience. 2009; 3
25. Presacco A, Goodman R, Forrester L, Contreras-Vidal JL. Neural decoding of treadmill walking from noninvasive electroencephalographic signals. Journal of neurophysiology. 2011; 106:1875–1887. [PubMed: 21768121]
26. Chéron G, Duvinage M, De Saedeleer C, Castermans T, Bengoetxea A, Petieau M, et al. From spinal central pattern generators to cortical network: integrated BCI for walking rehabilitation. Neural plasticity. 2012; 2012
27. Bulea TC, Prasad S, Kilicarslan A, Contreras-Vidal JL. Sitting and Standing Intention Can be Decoded from Scalp EEG Recorded Prior to Movement Execution. Frontiers in Neuroscience. 2014; 8 [2014-November-25]
28. Kilicarslan, A.; Prasad, S.; Grossman, RG.; Contreras-Vidal, JL. High accuracy decoding of user intentions using EEG to control a lower-body exoskeleton. Engineering in Medicine and Biology Society (EMBC), 2013 35th Annual International Conference of the IEEE; 2013. p. 5606-5609.
29. Nakagome, S.; Luu, TP.; He, Y.; Contreras-Vidal, JL. Brain-Computer Interfaces to Virtual Reality Environments for Rehabilitation of Motor Function: A Review; presented at the Conf Proc IEEE Eng Med Biol Soc; 2015. in press
30. He, Y.; Nathan, K.; Venkatakrishnan, A.; Rovekamp, R.; Beck, C.; Ozdemir, R., et al. An integrated neuro-robotic interface for stroke rehabilitation using the NASA XI powered lower limb exoskeleton. Engineering in Medicine and Biology Society (EMBC), 2014 36th Annual International Conference of the IEEE; 2014. p. 3985-3988.
31. Antonsson EK, Mann RW. The frequency content of gait. Journal of Biomechanics. 1985; 18:39–47. //. [PubMed: 3980487]
32. Wu W, Gao Y, Bienenstock E, Donoghue JP, Black MJ. Bayesian Population Decoding of Motor Cortical Activity Using a Kalman Filter. Neural Comput. 2006; 18:80–118. [PubMed: 16354382]
33. Li Z, O'Doherty JE, Hanson TL, Lebedev MA, Henriquez CS, Nicolelis MA. Unscented Kalman filter for brain-machine interfaces. PloS one. 2009; 4:e6243. [PubMed: 19603074]
34. Orsborn AL, Dangi S, Moorman HG, Carmena JM. Exploring time-scales of closed-loop decoder adaptation in brain-machine interfaces. Conf Proc IEEE Eng Med Biol Soc. 2011; 2011:5436–5439. [PubMed: 22255567]
35. Delorme A, Makeig S. EEGLAB: an open source toolbox for analysis of single-trial EEG dynamics including independent component analysis. Journal of neuroscience methods. 2004; 134:9–21. [PubMed: 15102499]
36. Patterson KK, Parafianowicz I, Danells CJ, Closson V, Verrier MC, Staines WR, et al. Gait Asymmetry in Community-Ambulating Stroke Survivors. Archives of Physical Medicine and Rehabilitation. 89:304–310. [PubMed: 18226655]
37. Patterson KK, Gage WH, Brooks D, Black SE, Mcllroy WE. Evaluation of gait symmetry after stroke: a comparison of current methods and recommendations for standardization. Gait Posture. 2010 Feb.31:241–246. [PubMed: 19932621]
38. Masiero S, Poli P, Rosati G, Zanotto D, Iosa M, Paolucci S, et al. The value of robotic systems in stroke rehabilitation. Expert review of medical devices. 2014; 11:187–198. [PubMed: 24479445]
39. Ertelt D, Small S, Solodkin A, Dettmers C, McNamara A, Binkofski F, et al. Action observation has a positive impact on rehabilitation of motor deficits after stroke. Neuroimage. 2007; 36:T164–T173. [PubMed: 17499164]

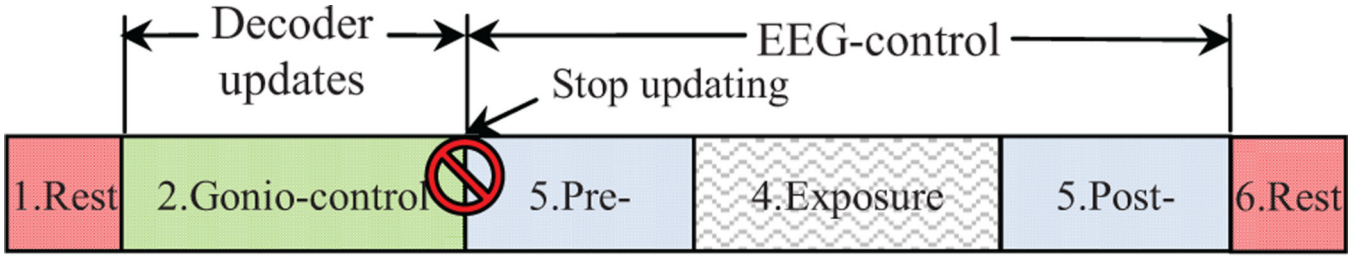

Phase	Actions	Duration (mins)
1	Rest.	2
2	Gonio-control: The avatar was driven by goniometer data. Decoder parameters were updated every 1 minute in this phase.	15
3	Pre-exposure: Right leg of the avatar was driven by decoder outputs.	8
4	Exposure: Decoder outputs were multiplied by perturbation gain, 0.7	15
5	Post-exposure: Perturbation gain was removed.	8
6	Rest.	2

Fig. 1.

The experimental procedures for each day. The time for each day is approximately 50 mins. Real-time decoding started 2 mins after starting the C++ program. Decoder parameters were updated every 1 minute and they were fixed by the end of *gonio-control*.

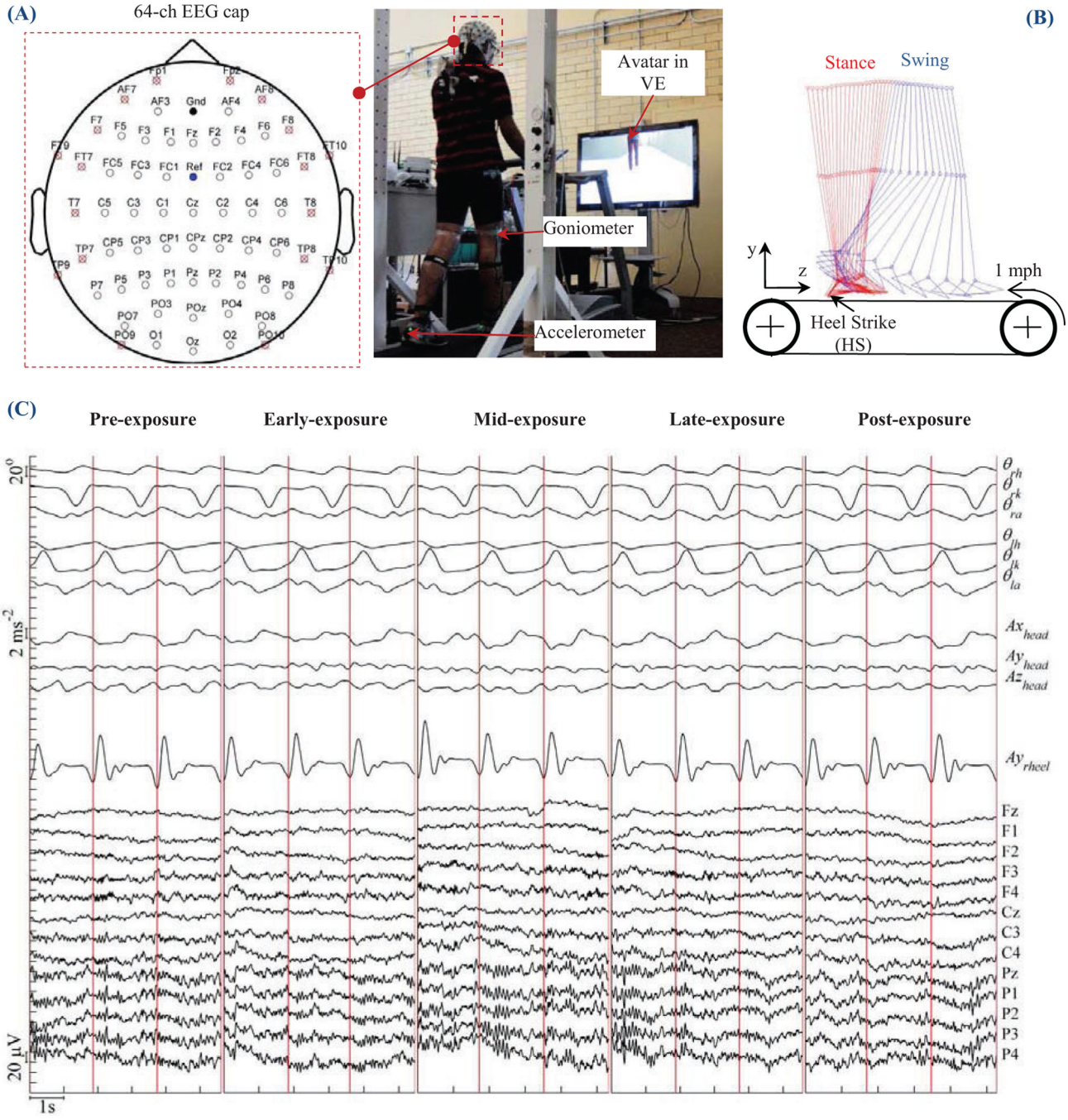

Fig. 2.

(A) Experimental setup in this study. Each subject was instructed to walk on a treadmill at 1 mph while looking at an avatar in a VE in front of them. Recorded data included electroencephlography (EEG), lower limb joint angles of both left and right leg, and accelerations of head, left heel, and right heel. Locations and EEG channel labels were also displayed. Channels marked with an "x" were not used in the decoder. (B) Illustration of a full walking gait cycle. (C) Raw data during pre-, early-, mid-, late- and post-exposure in one day.

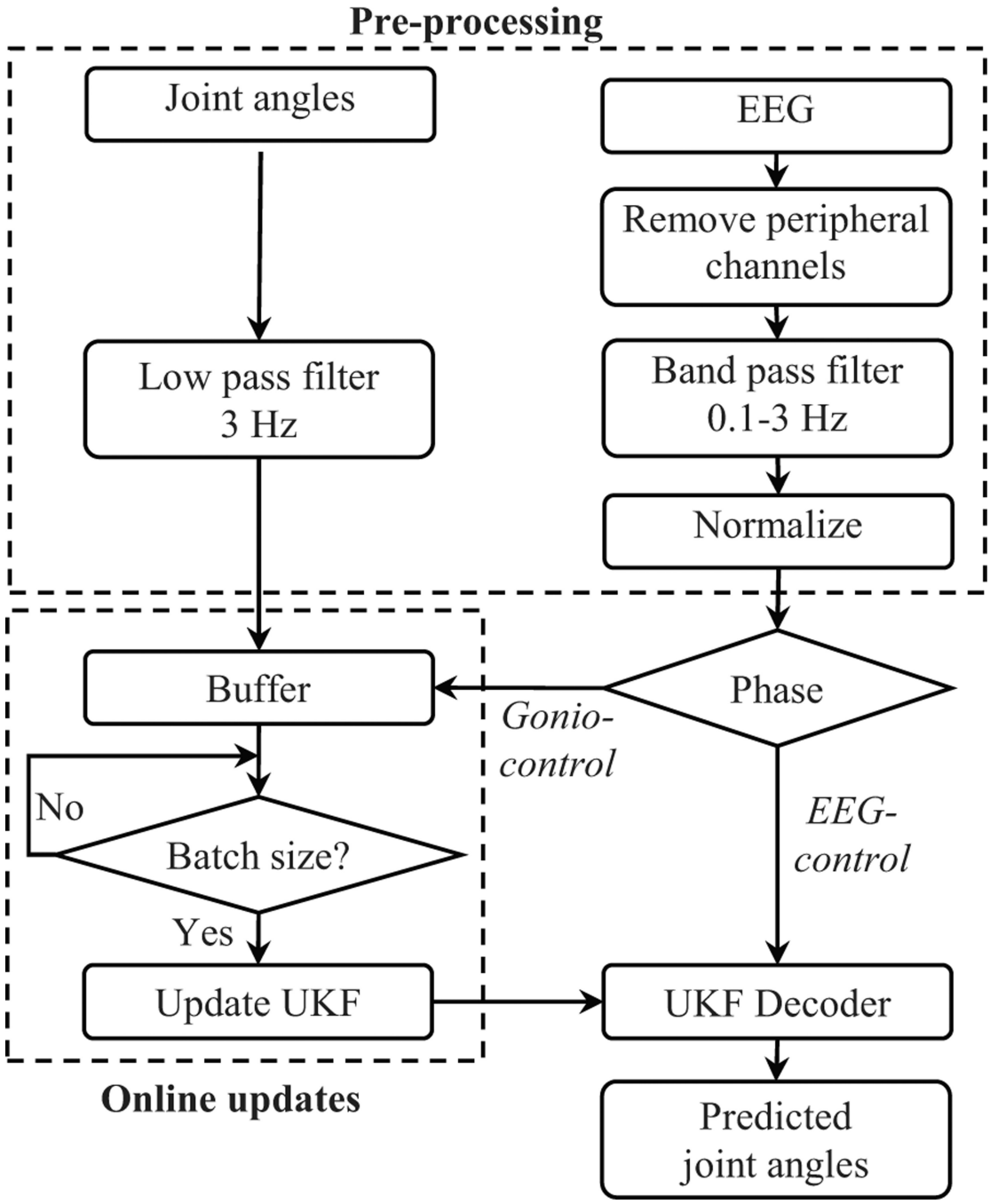

Fig. 3.
Flow chart of the signal processing, unscented Kalman filter parameters updates and avatar control used in this study.

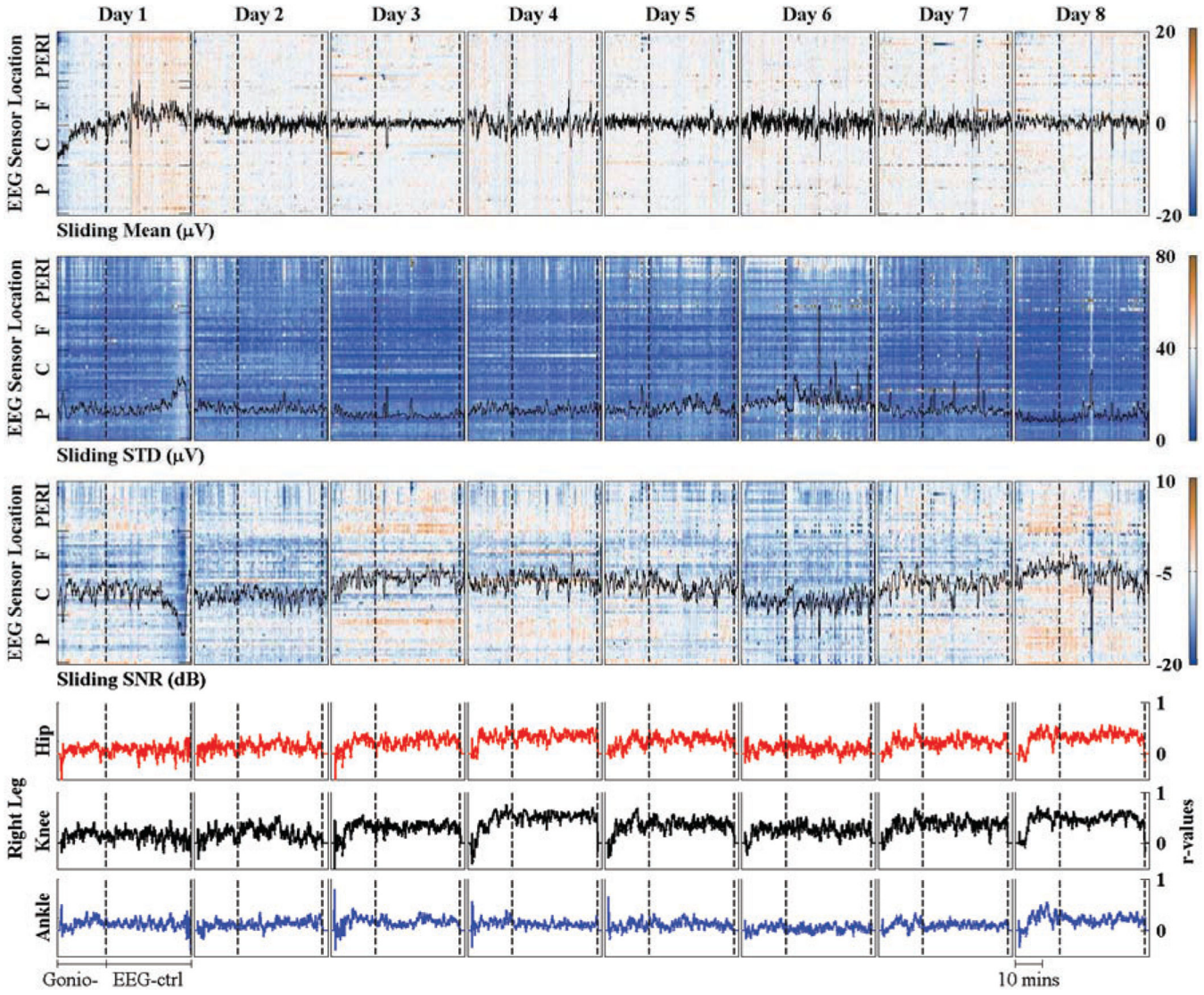

Fig. 4.

Mean, STD and signal to noise ratio (SNR) of EEG data of subject S2 across 8 days. The values were calculated from sliding windows (window size: 30s. and step size of Is). EEG channels were grouped into peripheral (PERI), Frontal (F), Central (C), and Post (P) location. Broken line divides each trial into *gonio-control* (Gonio-) and *EEG-control* (EEG-ctrl) mode, r-values between decoder outputs and actual joint angles are shown in the last row.

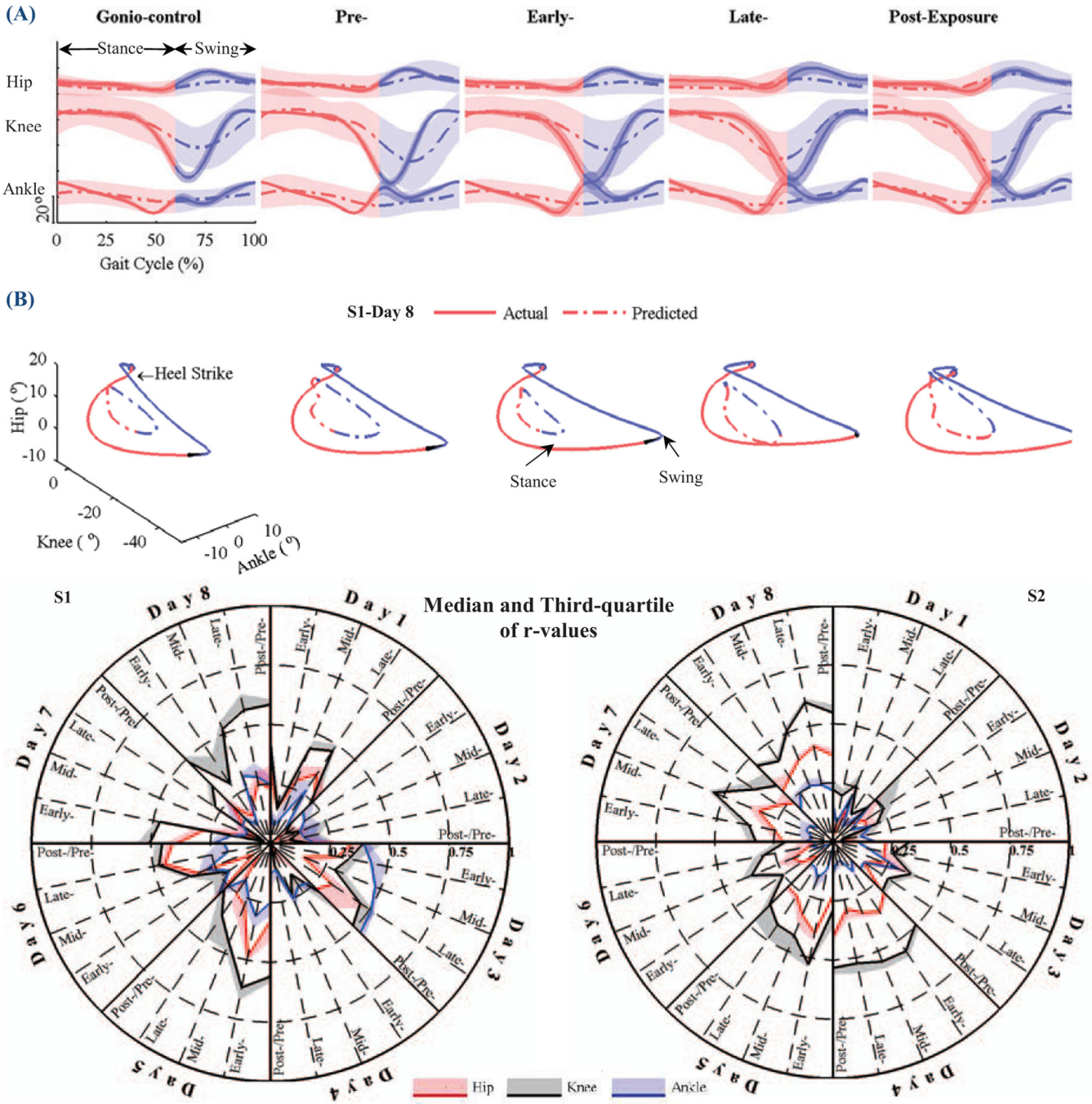

Fig. 5.

(A) Mean and standard deviation (STD) of actual and predicted lower limb joint angles of the right leg during gonio-control, pre-, early-, late- and post-exposure (Si-Day 8). (B) Actual and predicted 3D trajectories for lower limb joint angles. (C) Plots of Pearson's *r* of the predicted angles in each phase against the actual angles in *gonio-control* phase (baseline) for subjects SI and S2 in all days.

TABLE I

Pearson's r values for subjects S1 and S2.

Day	S1			S2		
	Hip	***Knee***	***Ankle***	***Hip***	***Knee***	***Ankle***
1	0.29±0.13	0.34±0.14	0.18±0.10	0.07±0.10	0.14±0.12	0.13±0.07
2	0.01±0.19	0.06±0.16	0.10±0.10	0.15±0.09	0.21±0.13	0.14±0.07
3	0.21±0.12	0.31±0.12	0.40±0.14	0.25±0.09	0.32±0.07	0.17±0.07
4	0.08±0.11	0.23±0.14	0.19±0.08	0.34±0.08	0.51±0.08	0.12±0.05
5	0.25±0.15	0.40±0.17	0.23±0.09	0.29±0.08	0.38±0.09	0.13±0.07
6	0.28±0.12	0.26±0.15	0.24±0.08	0.10±0.09	0.27±0.10	0.04±0.06
7	0.21±0.16	0.32±0.19	0.17±0.09	0.23±0.08	0.38±0.09	0.10±0.05
8	0.17±0.11	0.51±0.10	0.22±0.10	0.34±0.08	0.48±0.09	0.21±0.06

Values are mean ± standard devidation (STD)

TABLE II

Gait symmetry ratios (SRs) for all subjects across all days

Phase	S1			S2		
	Hip	***Knee***	***Ankle***	***Hip***	***Knee***	***Ankle***
1	0.96±0.25	0.99±0.36	0.88±0.14	0.94±0.14	1.02±0.13	0.84±0.12
2	0.82±0.48	0.86±0.48	0.79±0.41	0.58±0.36	0.67±0.40	0.57±0.33
3	0.57±0.36	0.61±0.34	0.54±0.28	0.41±0.25	0.48±0.29	0.38±0.24
4	0.52±0.30	0.56±0.31	0.53±0.27	0.42±0.25	0.50±0.29	0.39±0.21
5	0.54±0.33	0.60±0.35	0.53±0.26	0.43±0.24	0.52±0.30	0.41±0.23

Values are mean ± standard devidation (STD)

Int Conf Virtual Rehabil. Author manuscript; available in PMC 2016 October 04.